

Dynamical delocalization in one-dimensional disordered systems with oscillatory perturbation

Hiroaki Yamada

Faculty of Engineering, Niigata University, Ikarashi 2-Nocho 8050, Niigata 950-21, Japan

Kensuke S. Ikeda

Faculty of Science and Engineering, Ritsumeikan University, Noji-cho 1916, Kusatsu 525, Japan

(Received 20 August 1998)

The effect of dynamical perturbation on the quantum localization phenomenon in a one-dimensional disordered quantum system (1DDS) is investigated systematically by a numerical method. The dynamical perturbation is modeled by an oscillatory driving force containing M independent (mutually incommensurate) frequency components. For $M \geq 2$ a diffusive behavior emerges and in the presence of the finite localization length of the asymptotic wave packet can no longer be detected numerically. The diffusive motion obeys a subdiffusion law characterized by the exponent α as $\xi(t)^2 \propto t^\alpha$, where $\xi(t)^2$ is the mean square displacement of the wave packet at time t . With an increase in M and/or the perturbation strength, the exponent α rapidly approaches 1, which corresponds to normal diffusion. Moreover, the space-time (x - t) dependence of the distribution function $P(x,t)$ is reduced to a scaled form decided by α and another exponent β such that $P(x,t) \sim \exp\{-\text{const} \times (|x|/t^{\alpha/2})^\beta\}$, which contains the two extreme limits, i.e., the localization limit ($\alpha = 0, \beta = 1$) and the normal-diffusion limit ($\alpha = 1, \beta = 2$) in a unified manner. Some 1DDSs driven by the oscillatory perturbation in different ways are examined and compared.

[S1063-651X(99)05304-0]

PACS number(s): 05.45.-a, 72.15.Rn, 71.55.Jv, 71.23.-k

I. INTRODUCTION

The localization phenomena in one-dimensional disordered quantum systems (1DDS) have been extensively studied for several decades [1,2]. It is well known that almost all the eigenstates are localized under the presence of any disorder [3]. The detailed features of localization, of course, depend upon the nature of a random potentials, and the quantum diffusion of a wave packet in the 1DDS is in general suppressed within a finite length by the interference effect. The localization is regarded as a result of the coherent backscattering by irregularly distributed scatterers [2]. There are generally two length scales in the disordered quantum systems; one is the mean free path and the other is the localization length [4]. The time dependence of the mean square displacement (MSD) of an initially localized wave packet grows as t^2 within the mean free path. Such a growth is suppressed as the packet length reaches the second scale, i.e., the localization length [5]. Between the two scales, it is supposed that an intermediate regime exists in which the MSD grows according to a power law t^α ($0 < \alpha \leq 1$). However, the existence of such a diffusive regime has not been established in the ordinary 1DDS, since these two lengths are almost of the same scale [1,2]. Even in disordered systems of more than one dimension, for which the localization length may be much enhanced and may even become infinite, the existence of such an intermediate regime is not very clear, although some indications have been obtained [6,7]. Regardless, a finite localization length means that the memory on the initial state is maintained in the 1DDS even for a long-time scale, and there are no stochasticization processes which result in statistical behavior. In short, the 1DDS is not ergodic, and therefore exhibits no mixing property, i.e., no decay of correlation. Such features may be, however, drasti-

cally changed if the localized system is coupled with different dynamical degrees of freedom [8,9]. This is the subject we will discuss in the present paper.

An extreme case is that the 1DDS is coupled with a heat reservoir composed of an infinite number of degrees of freedom. In this case the influence from the heat reservoir is modeled by stochastic forces applied to each of the lattice sites [10,11]. Such a perturbation will destroy the quantum coherence which is the origin of the Anderson localization, and the wave packet diffuses beyond the intrinsic localization length. In most theoretical treatments the stochastic forces are modeled by Gaussian noise with a very short spatiotemporal correlation [12,13]. In such a class of stochastic lattice model a classical normal diffusion in which the MSD grows linearly with time occurs, as is naturally expected [12]. However, the diffusion coefficient is decided only by the parameters characterizing the statistical properties of the stochastic force and does not explicitly depend upon the length scales of Anderson localization. This fact implies that the generic dynamical structure inherent in the localization is entirely destroyed by the stochastic perturbation. In such class of models, the electronic stochasticization resulting in diffusion is "forced" by the externally introduced stochasticity.

A more interesting scenario of the electronic stochasticization is the possibility that the stochasticization mechanism is *spontaneously organized* in the system *without any help of the external stochastic source*. A possibly simplest situation is modeled by the 1DDS perturbed by a classical oscillating force with several frequency components. It is known that such a class of system is equivalent to an autonomous system, that is, the 1DDS coupled with linear oscillators with the same set of natural frequencies [14], and the linear oscillator can be identified with a highly excited quantum har-

monic oscillator [9]. Thus the proposed model may be looked upon as an isolated autonomous system composed of 1DDS and a finite number of linear oscillators.

A practical example of an oscillatory perturbation is the ac electric field. Mott and Davies discussed the conductivity of ac-driven disordered systems by using the Kubo-Greenwood formula [15,16]. Later, Wilkinson also dealt with the response of an electron to low frequency perturbation from the viewpoint of the nonadiabatic transition, which is different from Mott's theory [17]. However, they are both based upon the perturbation theories, and in applying the perturbation theories the stochasticization of an electronic state has implicitly been supposed. Indeed, the results of perturbation theories, which are based upon the short-time expansion, are significant only if any stochasticization mechanisms destroy the dynamical coherence within the time scale under consideration, but the origin of the stochasticization is not explained within the framework of the perturbation theories. On the other hand, Wilkinson concludes that the stochasticization in disordered quantum system is inhibited even if it is perturbed by an ac field, because of the localization effect in the adiabatic Floquet basis set [18]. The dynamical effects of the coherent oscillatory perturbations on the disordered electronic system are still very unclear.

On the other hand, the oscillatory perturbation may work for the electron as if there were a lattice vibration rather than a coherent ac field. Whether the oscillatory perturbation acts as if there is a coherent ac electric field or as if there is an incoherent lattice vibration will depend on the number of independent frequency components. In the present paper we systematically investigate the effect of oscillatory perturbations on the 1DDS. In particular, we are interested in how the number of frequency components, i.e., the number of degrees of freedom, composing the perturbation influences the dynamical properties of the system. In our preliminary reports, we have shown that the 1DDS is very sensitive to a coupling with systems with other degrees of freedom and that a periodically perturbed 1DDS exhibits a diffusive behavior over an unexpectedly long-time scale [8,9]. Decoherence in quantum systems induced by the coupling with other systems with a small number of degrees of freedom is an important subject in quantum phenomena [19–21]. In particular, there have been some examples of classically chaotic quantum systems (so-called quantum chaos systems) in which stochasticization is self-organized and the localizationlike effect can be destroyed spontaneously due to the coupling with a system with other degrees of freedom. For example, classical chaotic diffusion, which is suppressed by an Anderson localizationlike mechanism in the corresponding quantum systems [22], can be restored by a very weak coupling with systems with other degrees of freedom [23–27], which implies that the localization effect is very weak against a coupling with systems with other degrees of freedom. In the case of kicked rotators, the coupling with oscillatory perturbation is roughly equivalent to an increase in the spatial dimension and transition to the delocalization is observed [24,25,34,35].

More generally, whether the classical counterpart of a quantum chaos system exhibits diffusion is not essential: any quantum chaos system may restore the mixing properties through a phase-transition-like behavior by a very weak

(more precisely, decided by \hbar and thus classically negligible) coupling with a small number of linear oscillators [28].

We may thus expect that a similar stochasticization mechanism is “self-organized” in the Anderson localized 1DDS when it is coupled with some other degrees of freedom. On the other hand, it should be noted that the 1DDS is essentially different from the quantum chaos systems in the following sense: the latter have their classical counterparts exhibiting a well-defined normal diffusion, or more generally, the mixing properties in the limit of $\hbar \rightarrow 0$, but the former in general do not have such classical counterparts. Thus the stochastic behaviors which might be realized in the dynamically perturbed 1DDS will be different from those observed in the quantum chaos systems.

In the present paper we numerically investigate the time evolution of the wave packet in 1DDS under the presence of oscillatory perturbations and investigate how the effect of the perturbation changes the fundamental nature of Anderson localization. It is shown that the perturbation drastically increases the localization length up to a level undecidable by numerical calculations and a diffusion behavior is observed over a wide range of the control parameters. The main result is that the diffusion is not a normal diffusion but an anomalous diffusion, and moreover the spatiotemporal behavior of the probability distribution function is reduced to a simple scaling form. The outline of the present paper is as follows.

In Sec. II the model system investigated in the present paper is introduced. The model system is a one-dimensional tightly binding system perturbed by an oscillatory force composed of incommensurate frequency components of the basic model which are also discussed, and the method of numerical simulation is explained briefly.

In the next section, we investigate the wave packet dynamics exhibited by the basic model system. First, we show that the localization length is enhanced but is finite in the case of monochromatic perturbation. However, if the number of frequencies is more than one, the localization length is drastically enhanced to a level undetectable by the numerical method. It is shown that the wave packet spreads without limit according to an anomalous diffusion process characterized by a certain exponent. How the characteristics of such an anomalous diffusion depend on control parameters such as the perturbation strength and the number of incommensurate frequencies is explored in detail. The latter half of Sec. III is devoted to the spatiotemporal characterization of the probability distribution function which is responsible for the anomalous diffusion. Analyzing the results of extensive numerical simulation it is found that the probability distribution function reduces to a scaling form, which is characterized by two exponents: one is the exponent of the anomalous diffusion, and the other is an exponent describing the spatial decay of the distribution function. The scaling function has a “unified form” in the sense that it contains the two cases, i.e., the Anderson localization and the normal diffusion as the two extreme limits.

Finally, in Sec. IV, some other models different from the basic model in the scheme of the coupling with the oscillatory perturbation are examined, and the diffusion properties are investigated in comparison with the basic model investigated in Sec. III.

The last section is devoted to summaries and discussions.

II. MODELS AND METHOD OF SIMULATION

A. Models

The model we consider in the present paper is a one-dimensional tightly binding electronic system perturbed by periodically oscillating forces. The Hamiltonian is given by

$$H(t) = \sum_{n=1}^N |n\rangle [V_0(n) + V_1(n,t)] \langle n| + \sum_{n \neq m}^N |n\rangle K(n,m) \langle m|, \quad (1)$$

$$V_1(n,t) = V_1(n) \frac{\epsilon}{\sqrt{M}} \sum_{j=1}^M \cos(\omega_j t). \quad (2)$$

The basis set $\{|n\rangle\}$ is an orthonormalized one representing lattice sites, and $V_0(n)$ and $V_1(n)$ are the on-site energies of an electron at the site n , $V_0(n)$ varies at random in the range $[-W, W]$ from site to site, and the transfer energy vanishes unless sites n and m are adjacent [$K(n,m) = \delta_{n,m \pm 1}$]. The strength of the site energy is fixed mainly at $W=0.9$ throughout the present paper, and we set $\hbar = 1$ without loss of generality. We set the system size and ensemble size 1024 and 20–50, respectively, throughout the present paper.

The oscillatory perturbation is polychromatic and is composed of M different frequency components (colors), and the frequencies $\{\omega_j\}$ are chosen to be mutually incommensurate, and are typically given as $\omega_1 = 1$, $\omega_2 = 1 + \sqrt{\frac{2}{25}}$, $\omega_3 = 1 + \sqrt{\frac{3}{25}}$, \dots , and so on.

As is shown by Eq. (2), we have supposed that all the amplitudes of the periodic components have the same value, and ϵ characterizes the strength of the oscillatory perturbation. In fact, the long-time average of the squared perturbation amplitude is given by

$$\langle V_1(n,t)^2 \rangle_t / V_1(n)^2 = \frac{\epsilon^2}{2}, \quad (3)$$

where $\langle \rangle_t$ indicates the long-time average. We are interested in how the periodic perturbations influence the quantum nature of the 1DDS as the number of colors M and/or the perturbation strength ϵ are changed.

We are most interested in how the oscillatory perturbation $V_1(n,t)$ influences the localization phenomena due to the randomness of the on-site potential $V_0(n)$, which we call the *perturbed localization problem*. To investigate this kind of problem, we may choose the simple form of the perturbation,

$$V_1(n) = V_0(n). \quad (4)$$

We call this model the localization model (L model) because the Anderson localization dominates in the limit of $\epsilon \rightarrow 0$. Most of the present paper is devoted to the study of the L model. A similar model with oscillatory perturbation applied to the off-diagonal part has been used by several authors [34,35].

We can also study other physical situations with our model (1), (2). In the limit

$$V_0(n) = 0, \quad (5)$$

the system becomes the free electron model if the oscillatory perturbation is switched off. By switching on $V_1(n,t)$ our model describes a free electron scattered by quasiperiodically oscillating irregular potentials. This situation is also interesting as it is connected with the problem of a ballistic electron scattered by dynamical impurities. We refer to this model as the ballistic model (B model).

In addition to these two cases, we can consider a particular case where the perturbation amplitude does not vary irregularly from site to site but depends systematically on the sites as

$$V_1(n) = n. \quad (6)$$

We call such a model the AC model, because the periodic perturbation models the effect of an ac electric field. With this model we can study how localization is influenced by a polychromatic ac field. There have been some studies on the diffusion of the electrons under the influence of the ac field, but the time-dependent perturbation theory [15] or the adiabatic perturbation theory have been used in these treatments [17]. Such theories implicitly assume the destruction of dynamical coherence in the system and cannot deal with the fully dynamical evolution process. Very recently, Diez *et al.* have investigated the time-dependent property of an electron in a semiconductor superlattice with disorder driven by an ac electric field, as a realistic model [36]. Whether an intrinsic diffusion occurs in the 1DDS with the ac field is still an open problem.

We numerically investigate the AC model in Sec. IV in comparison with the L model.

B. Method of simulation

We numerically integrate the following time-dependent Schrödinger equation under periodic boundary conditions:

$$-i \frac{\partial \Psi(n)}{\partial t} = \Psi(n+1) + \Psi(n-1) - V(n,t) \Psi(n). \quad (7)$$

The Planck constant \hbar is chosen to be 1 without loss of generality. We explain the method of integration we have used in this paper briefly. By using the continuum coordinate \hat{x} and the momentum operator $\hat{p} = -i \partial / \partial x$ in Eq. (7) the Hamiltonian is rewritten as

$$\hat{H}(t) = e^{\partial / \partial x} + e^{-\partial / \partial x} + V(x,t) \equiv \hat{T} + \hat{V}(t), \quad (8)$$

where

$$\hat{T} = 2 \cos(\hat{p} / \hbar), \quad \hat{V} = V(\hat{x}, t). \quad (9)$$

The wave function $\Psi(x,t)$ at the site x and the time t is expressed by using a time evolution operator,

$$\Psi(x,t) = \hat{U}(t,0) \Psi(x,0) \quad (10)$$

$$= T_+ \exp \left(-\frac{i}{\hbar} \int_0^t dt' \hat{H}(t') \right) \Psi(n,0), \quad (11)$$

where T_+ is the time ordering operator. It is known that by using the Baker-Hausdorff-Campbell theorem the unitary operator \hat{U} can be approximated by an operator given by an alternative product of the p -dependent operator and x -dependent operator:

$$\hat{U}(\Delta t, 0) \approx \prod_i^k \exp(c_i \hat{T}) \exp[d_i \hat{V}(x, e_i \Delta t)], \quad (12)$$

where the coefficients $e_i = \sum_{j=1}^i c_j$. If the set of the coefficients c_i and d_i is chosen appropriately, the error of the product operator can be made as small as $O(\Delta t^{k+1})$. See Refs. [29–33] for the details of the coefficients. Such a numerical scheme of integration is called the k th-order symplectic integrator (SI) scheme and it enables us to do the numerical integration of the Schrödinger equation at an extremely high numerical accuracy. Further, another advantage of using such an operator is that the norm of the wave function is exactly conserved because it is a unitarity operator.

The numerical procedure of operating the SI can be drastically sped up by using the fast Fourier transformation (FFT) and the inverse FFT. When an x -dependent operator is applied, the wave function is represented by the coordinate (x) representation in which the x -dependent operator is diagonal. After applying the x -dependent operator, the wave function is transformed into the p -represented one by using the FFT, and the p -dependent operator is operated on the diagonal form. Finally the resulting wave function is transformed back into the x representation by the inverse FFT. By repeating such procedures numerically, a single operation of the SI is achieved. Since our system is defined on a discrete lattice, if we take the number of lattice sites $N=2^m$ (m : positive integer) and impose the periodic boundary condition, the FFT and the inverse FFT can be executed exactly except for round-off errors. This is the remarkable advantage of applying the FFT-SI scheme to our lattice problem. As the k th-order SI scheme is composed of $2^{k/2}x$ and p operators and the CPU time for a single application of the FFT algorithm is proportional to $N \ln N$, the CPU time required for a single step of the k th-order FFT-SI scheme is estimated as $N \ln N \times 2(2^{k/2} - 1)$. See Ref. [33] for more detailed information on the computer performance of the FFT-SI scheme.

As mentioned above, no significant error emerges at the FFT and the inverse FFT. Thus the numerical error comes only from the approximation by the symplectic integrator. The accumulated error during the ℓ step iteration of the k th-order SI is expected as $E_k(\ell) \propto (\Delta t)^{k+1} \ell$. The error is predominantly controlled by the size of time step, but there are some other extra factors that significantly influence the accumulated error, for example, the amplitude of the on-site irregular energy.

We compare in Fig. 1 some typical numerical results obtained by using the FFT-SI schemes of different order with several magnitudes of the time step in order to demonstrate how we have decided the size of the time step and the order of the SI scheme. Here we used the L model without the oscillatory perturbations ($\epsilon=0$), and so the wave function is Anderson localized. Figure 1 shows the time dependence of the mean square displacement for typical samples calculated by second- and sixth-order SI schemes at a relatively large

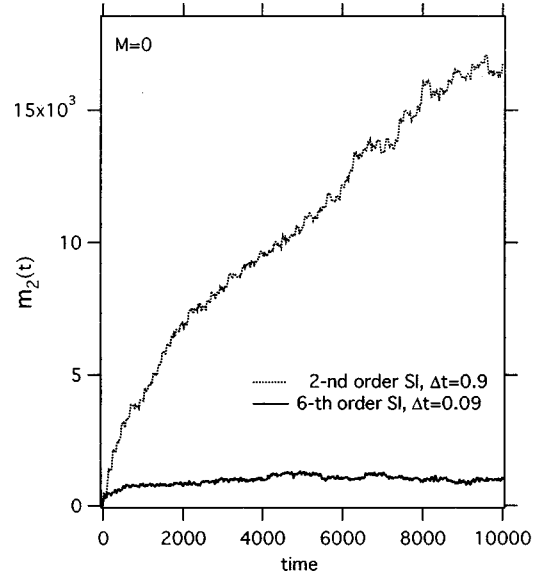


FIG. 1. Time dependence of square displacements for a sample of L model without perturbation. We use second-order and sixth-order SI schemes with time mesh $\Delta t=0.9$.

size of time step, $\Delta t=0.9$. It is obvious that the wave packet spreads more than the case of the sixth-order scheme if the second-order SI scheme is used.

Further, we have confirmed that the latter temporal evolution of MSD coincides with one obtained at the smaller size of time step, $\Delta t=0.05$, and further decrease in the size of time step no longer gives significant change in the time-evolution data. Note also that even the second-order scheme almost reproduces the result of the sixth-order scheme at $\Delta t=0.05$. From these results, we can conclude that the sixth-order FFT-SI scheme at $\Delta t=0.05$ achieves a reliable numerical accuracy. The advantage of our model is that the numerical simulation can be done precisely over a very long-time scale because of the one-dimensional nature of our model, and quantitatively accurate information on the quantum diffusion of the wave packet can be obtained.

It is also worthwhile to note that the eighth-order scheme is not effective for the calculations at double precision. If quadruple precision is available in the numerical simulation, the eighth-order scheme might become more efficient.

III. DYNAMICAL DELOCALIZATION

In this section we present a systematic investigation of the diffusion properties of the L model. We only consider time evolution in which the wave front of the packet does not reach the boundary in order to avoid the influence of boundary condition and finite size effect. In fact, extending the system size has confirmed that the boundary condition has no effect in some cases. This will also be confirmed by the shape of the wave packet reported in Sec. III D.

A. Monochromatic perturbation ($M=1$)

To observe the temporal behavior of the electronic wave function in the L model, we monitor the time dependence of mean square displacement of the wave packet;

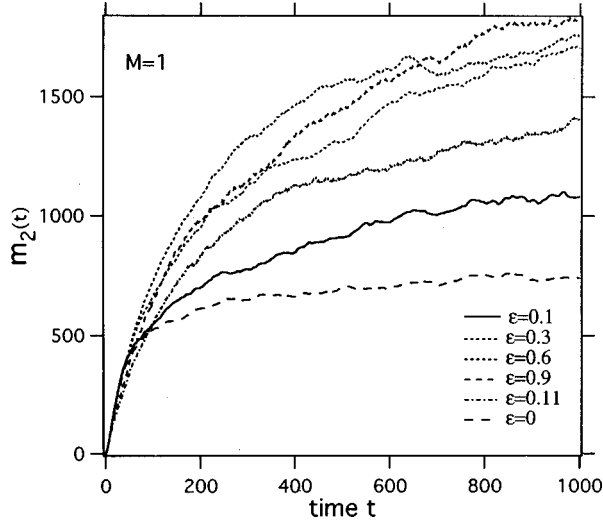


FIG. 2. (a) Time dependence of MSD in cases driven by monochromatic perturbation ($M=1$) with some perturbation strength.

$$m_2(t) = \xi(t)^2 \equiv \langle \langle \Psi(t) | (\hat{n} - \langle \hat{n} \rangle)^2 | \Psi(t) \rangle \rangle_{\Omega}, \quad (13)$$

where $\hat{n} \equiv \sum_{n=1}^N n |n\rangle \langle n|$ is the position operator, and the angle brackets, $\langle \rangle$, $\langle \rangle_{\Omega}$, mean the quantum and the ensemble averages, respectively. Usually we take the ensemble average over 20 different samples.

We first investigate the perturbation strength dependence of the MSD as a function of time in the case of monochromatic perturbation ($M=1$). Figure 2 shows the MSD and its logarithmic plots at several perturbation strengths. Apparently the wave packet spreads beyond the width of the asymptotic wave packet of the unperturbed case (i.e., $\epsilon=0$). Observing the diffusive behavior in more detail, the increasing rate of MSD seems to be suppressed as the time elapses.

To confirm whether the diffusive behavior continues or not, we examined a simulation on an extremely long-time scale by using a larger size of time step, $\Delta t=0.5$, which is the upper limit that can reproduce the reliable data (typically the data at $\Delta t=0.05$ in Fig. 2). Figure 3 shows the result. Evidently, the diffusive behavior on the earlier time scale shown in Fig. 2(b) saturates at a certain level, and we have to conclude that the localization is not destroyed by the monochromatic perturbation. However, we stress that the localization length of the asymptotic wave packet is much enhanced by the monochromatic perturbation. Here we show in Fig. 3(b) the ϵ dependence of the enhanced localization length obtained from the data of Fig. 3(a). First, as the perturbation strength increases, the enhanced localization length also increases. However, when the strength exceeds a certain level, the increase of the localization length of the asymptotic wave packet is suppressed and the localization length in turn begins to decrease. As will be shown later, the suppression of the enhancement of the localization length of the asymptotic wave packet in the larger ϵ regime is a general feature of the L model.

Finally we comment on the relation between the present results and the ones presented in our preliminary report [8]. In a report we dealt with the same model in a slightly differ-

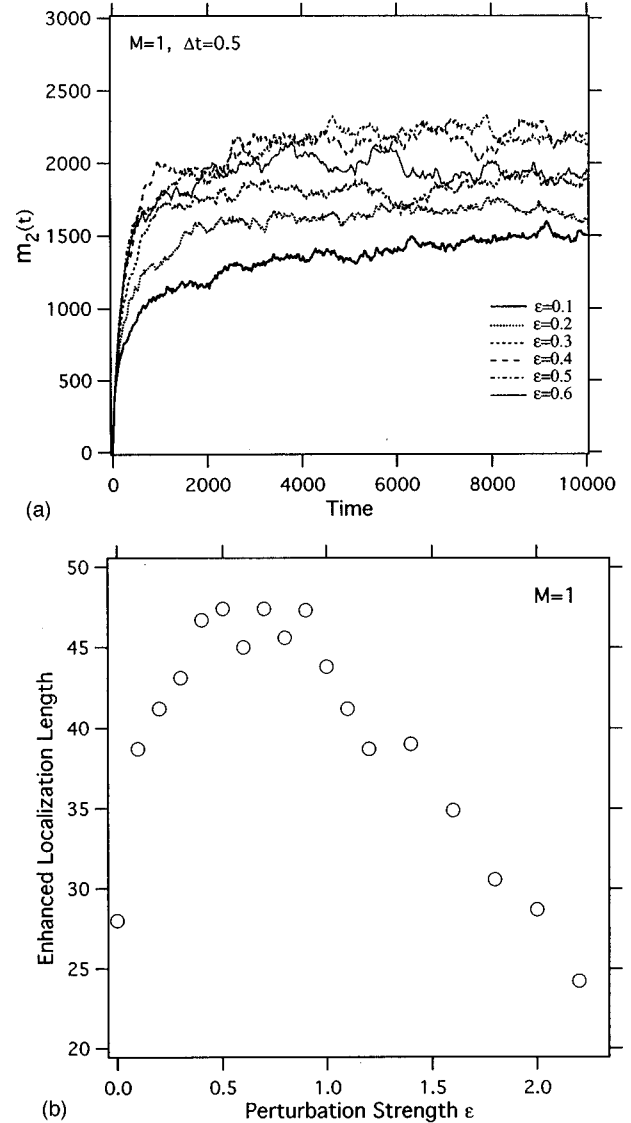


FIG. 3. (a) Same data as Fig. 2 except for the size of time step $\Delta t=0.5$. (b) The ϵ dependence of the enhanced localization length estimated by MSD in (a). The estimation of enhanced localization length of the asymptotic wave packet is based on time average for an interval ($T=8000-10000$) after saturation.

ent condition, and we concluded that the time dependence of the MSD is a normal diffusion. (Precisely, the initial phase of the perturbation was different.) However, the time scale of the numerical simulation is much shorter than the present simulation, and so the conclusion is not correct, but the early-stage temporal diffusion coefficient decided in the diffusive time scale in the preliminary report provides some insight into the dynamical feature of the monochromatically perturbed 1DDS. In fact we numerically estimated the perturbation strength dependence, and found that the diffusion coefficient does not obey $D \propto \epsilon^2$, and this fact implies that even the early-stage diffusion cannot be explained by the perturbation theory, which has been used by several authors [15,18].

An important property of the monochromatically perturbed system is that, unlike the 1DDS without the dynamical perturbation, the two fundamental scales, i.e., the mean free path and the localization length, seem to be well separated, and between the two scales the MSD exhibits a diffu-

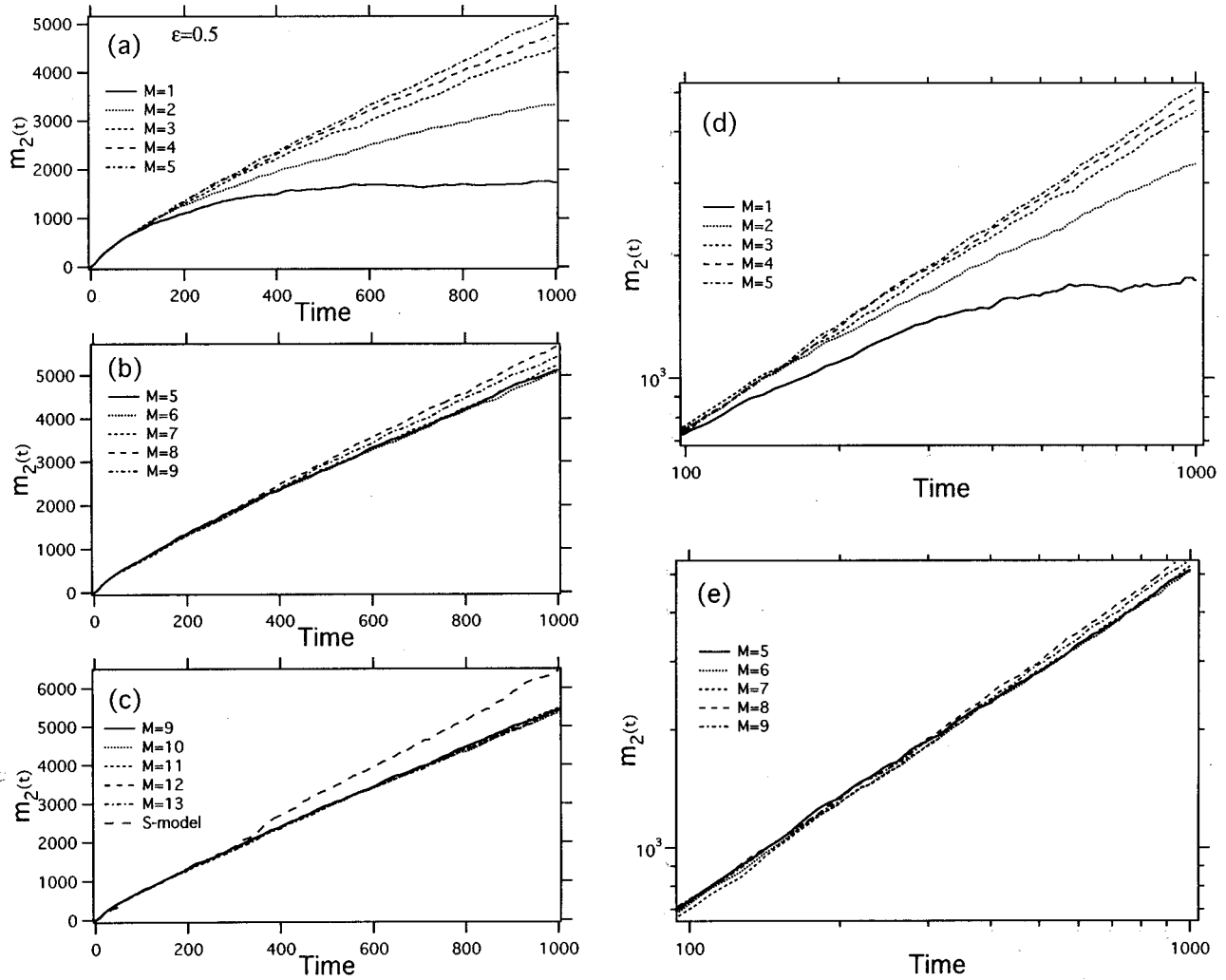


FIG. 4. (a)–(c) Time-dependent MSD of L model for polychromatic color ($M = 1$ – 13) at the perturbation strength, $\epsilon = 0.5$, and (d), (e) its logarithmic plots.

sive behavior. This is the reason a diffusive behavior is observed in our preliminary report. Precisely, the early-stage diffusion is not a normal diffusion. Indeed, Fig. 2(b) demonstrates that the logarithmic plots of MSD vs time are on straight lines in the early stage, but the tangents of the straight lines are all less than 1. This fact means that the transient diffusion is a subdiffusion rather than a normal diffusion. We note that all the features of diffusion are very similar to the ones observed in a 2DDS, where the two length scales are well separated [1,6]. Subdiffusion is a major characteristic of the diffusion process observed when the number of frequencies M is increased to more than one. This will be discussed in detail in the next subsection.

We have shown that a localization in 1DDS is sensitive to the external monochromatic perturbation, but the monochromatic perturbation is not adequate for destroying the localization perfectly.

B. Polychromatic perturbation ($M \geq 2$)

The question we examine in the present subsection is how the temporal behavior of MSD changes when the oscillatory perturbation contains more than one frequency component. First we investigate the change of temporal behaviors of

MSD as the number of frequencies (colors) is increased with the perturbation strength being kept at a relatively small fixed value ($\epsilon = 0.5$). In Figs. 4(a)–4(c) the time dependence of the MSDs is shown for the several polychromatic perturbations with different numbers of colors ($M = 1, 2, \dots, 13$). It is obvious that the wave packet, which is localized without the perturbations, spreads beyond even the enhanced localization length of the asymptotic wave packet of the monochromatically perturbed 1DDS ($M = 1$). As the number of frequencies M increases, the diffusion of the wave packet is more enhanced.

The increasing rate of MSD increases monotonically with the number of colors M , but it begins to be suppressed as M exceeds 3, and begins to saturate above $M \sim 5$. It seems that unlike the cases of monochromatic perturbation the diffusive behavior continues, and that no indication of localization is observed at least within the time scale we examined in the numerical simulation. Absence of localization has been confirmed for some M 's by extending the time scale of simulation up to $T = 10\,000$ [$m_2(t) \sim 40\,000$].

Although the MSD seems to increase without limit, the increasing rate of MSD in general decreases as the time elapses, and so the local diffusion coefficient decreases

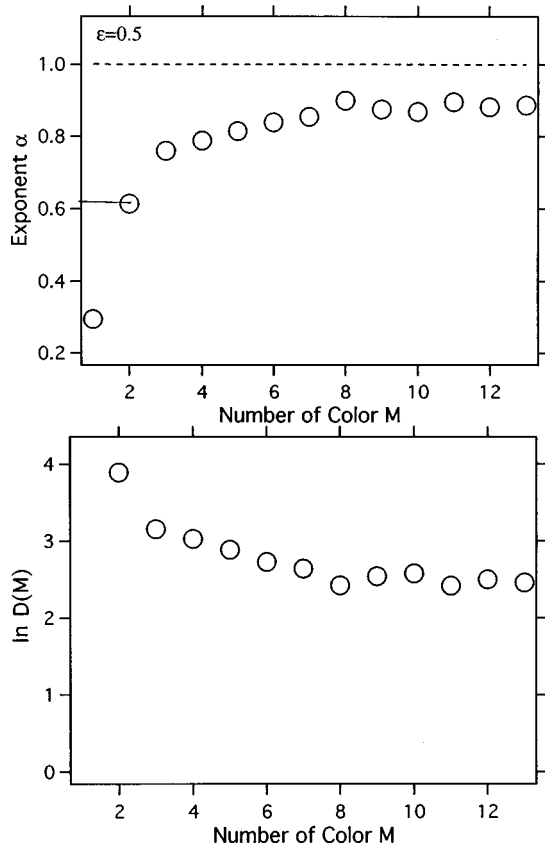


FIG. 5. Number of frequency dependence of (a) the power index α , and (b) coefficient D , estimated by the data in Fig. 4.

gradually in time. To investigate the nature of diffusion in more detail we show in Figs. 4(d) and 4(e) the logarithmic plot of MSD versus time. Except for the initial regime of time evolution where the transient effect still remains, all the data except for $M = 1$ align along straight lines with tangents less than 1, and so we may conclude that the MSD obeys a well-defined subdiffusion law:

$$m_2(t) = Dt^\alpha \quad (0 < \alpha < 1). \quad (14)$$

The subdiffusion shown in Fig. 4 is qualitatively different from the one observed in the monochromatic case in the sense that the localization length of the asymptotic wave packet seems to be infinite, or, that is, at least, drastically larger than the monochromatic case. The exponent α together with the coefficient $\ln D$ are estimated from Fig. 4. In the numerical fitting we used the least squares fit, discarding the data points in the very early stage of time evolution ($t < 100$), which is influenced by the initial phase of the perturbation.

Figure 5 shows the numerically estimated results of α and $\ln D$. We find that the exponent α gradually increases and approaches a constant value slightly less than 1. As will be shown below, the limiting value α approaches 1.0 in the limit of $M \rightarrow \infty$ if the perturbation strength ϵ is taken to be some finite value. Thus we may say that the subdiffusion tends to approach the normal diffusion, as the number of frequencies M increases. We have confirmed that the same behavior is also observed for other sets of values of the frequencies.

Note that it is difficult to judge exactly whether such a subdiffusion is endless or a transient phenomenon by numerical results even if we performed the larger scale simulation. As we mentioned in the Introduction, the number of frequency components can be regarded as the number of linear oscillators coupled to the 1DDS [28,9]. Accordingly, this result, that the localization can be destroyed by perturbation with two frequencies, is consistent with the appearance of an irreversible phenomenon reported in a previous paper [9].

It will be instructive to compare the above diffusion process with the stochastically perturbed diffusion process, where a stochastic perturbation is applied instead of the polychromatic perturbations. (We hereafter call the stochastically perturbed model the S model.) The MSD for the stochastic perturbation is shown in Fig. 4(c) as a reference. In the limit of $M \rightarrow \infty$ the diffusion of the polychromatically perturbed system approaches the one driven by the stochastic perturbation provided that the perturbation strengths ϵ are the same. Such a feature is comprehensible considering that the polychromatic perturbation can be identified with a white noise (or a colored noise if the frequencies are distributed over a finite bandwidth) in the limit of $M \rightarrow \infty$.

We conclude that even though the perturbation strength ϵ is not very strong, the Anderson localization seems to be destroyed if the number of colors is more than 1. Even if the localization is not destroyed, the localization length of the asymptotic wave packet is extremely enhanced, to a level undecidable by numerical simulations. The dynamical evolution in the delocalized regime occurs according to a well-defined subdiffusion process, and no sudden transition to normal diffusion can be observed as the number of colors is increased. Normal diffusion seems to be realized only in the large limit of the incommensurate color number M .

Before closing this subsection we remark on the ensemble average over the different samples. In the subdiffusion regime each sample is accompanied by a considerable number of fluctuations, and the time dependence of various quantum mechanical averages of a single sample does not give a significant result. We usually take the ensemble average over 20–50 different samples. Such a fluctuation, however, decreases in the normal-diffusion limit. This fact implies that the large fluctuation is strongly related to the nature of subdiffusion itself. The interesting statistical property of the sample-to-sample fluctuation in width of wave packet has been investigated for band random matrix models [37]. In order to make clear the relation with our model, we have to do numerical simulation for a large number of samples. The relation between the anomalous fluctuation and the subdiffusion will be investigated elsewhere [38].

C. Perturbation strength dependence

In this subsection, we investigate in detail how the transition from the subdiffusion to the normal diffusion takes place as the perturbation strength is varied continuously. Since we are interested mainly in the ϵ dependence, the color number is fixed to some representative values, i.e., $M = 2, 5, \text{ and } 10$.

Figures 6–8 show the time dependence of the MSD and its logarithmic plots at several perturbation strengths. From the logarithmic plots shown in Figs. 6–8 we can observe that

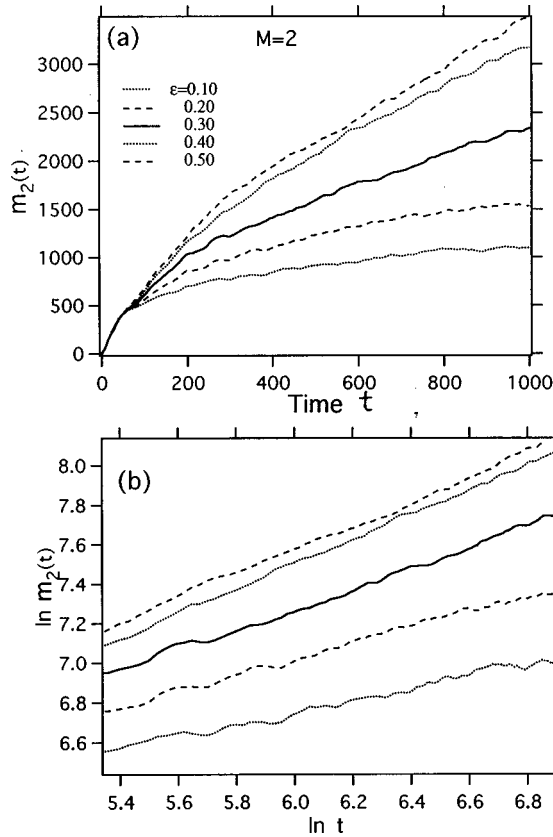


FIG. 6. (a) Time dependence of MSD in L model for the perturbation ($M=2$) at some perturbation strength and (b) its logarithmic plots.

even though the perturbation contains many frequency components, the diffusion process obeys the subdiffusion laws when the perturbation strength is small enough. This fact implies that, however large the number of frequencies may be, the polychromatic perturbation cannot also yield normal diffusion provided that the perturbation strength is weaker than a characteristic strength determined by the number of colors. (It will get smaller as the number M increases.) This is an essential feature different from the stochastic perturbation which induces a normal diffusion however small the strength ϵ may be.

In Fig. 9 the ϵ dependence of the numerically estimated exponent α of subdiffusion for the three cases $M=2$, 5, and 10 is shown. In all cases the exponent α increases steeply as ϵ increases, and eventually approaches unity, which means the onset of normal diffusion. As the number M increases, the approach to $\alpha=1.0$ with an increase in ϵ becomes faster. We stress again that the transition from subdiffusion to normal diffusion is continuous, and there seems to be no drastic change.

A more basic question is whether there is any transition from the localized state to the delocalized state in the extremely weak ϵ regime. This is a very hard question which is not easy to answer from the results of numerical investigations. The fact we could confirm is that for all the data points displayed in Figs. 6–8 the subdiffusion does not saturate up to the numerically computable time scale (up to $t \leq 10^4$).

Next we investigate how the spreading velocity of the wave packet depends upon the perturbation strength. Since

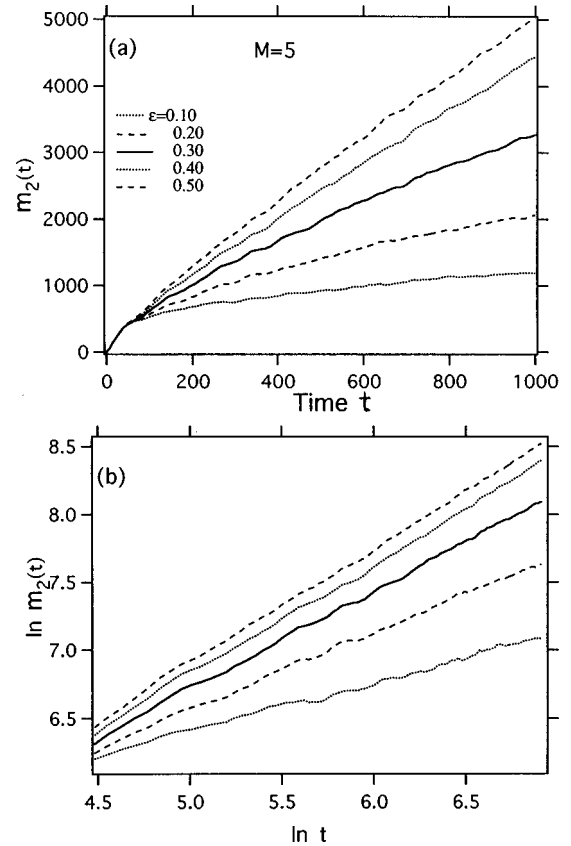


FIG. 7. (a) Time dependence of MSD in L model for the perturbation ($M=5$) at some perturbation strength and (b) its logarithmic plots.

our system exhibits subdiffusion, it is not possible to introduce some constant which quantitatively characterizes the spreading velocity throughout the diffusion process. The coefficient D introduced by Eq. (14) coincides with the diffusion constant in the normal-diffusion regime, but it does not directly characterize the spreading velocity in the subdiffusion regime. We, therefore, use the local diffusion rate $D(T, \Delta T)$, which is decided by the tangent of the least squares fit to the data for the finite-time interval $T \leq t \leq T + \Delta T$. In Figs. 10(a) and 10(b) we depict the ϵ dependence of the local diffusion rates $D(T, \Delta T)$ measured at $T=100$, 300, 500, and 700 for the interval $\Delta T=200$. A remarkable fact is that they first increase rapidly and reach a maximum value and finally decrease slowly. The value of ϵ which makes the local diffusion rate $D(T, \Delta T)$ maximum almost agrees with the characteristic value at which the index α begins to saturate to 1.0 (see Figs. 6–8). As has been mentioned in Sec. III A, similar characteristics are observed for the monochromatic perturbation system in the ϵ dependence of the enhanced localization length.

To have some idea of such a characteristic behavior, we compare the above results with the diffusion rate of the 1DDS perturbed by the stochastic perturbation [see Figs. 11(a) and 11(b)]. Figure 12 shows the ϵ dependence of the diffusion rate numerically estimated from MSD. The global feature of the ϵ dependence is very similar to the results shown in Fig. 10(a). In particular, the values of ϵ^* (≈ 1.0) which make the diffusion rates maximum coincide and the maximum values of the local diffusion rates are also close to

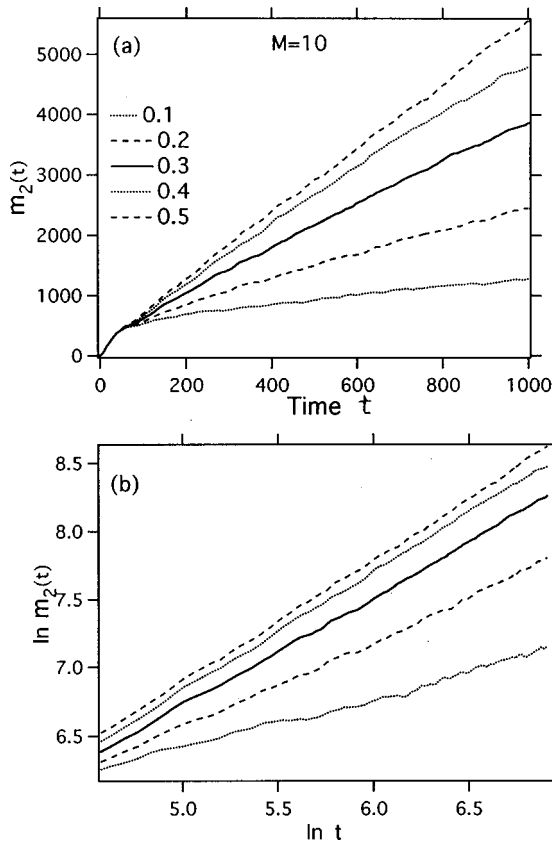


FIG. 8. (a) Time dependence of MSD in L model for the perturbation ($M=10$) at some perturbation strength and (b) its logarithmic plots.

each other. However, the detailed behaviors exhibit significant differences. In the very small regime of ϵ , the diffusion rate behaves as $D(\epsilon) \propto \epsilon^2$ in the case of stochastic perturbation, while it seems to grow linearly rather than as ϵ^2 in cases of polychromatic perturbation. Further, in the larger ϵ regime, $D(\epsilon)$ seems to decay $\propto \epsilon^{-2}$ in the stochastic case, but $D(\epsilon)$ decays more slowly in the polychromatic case. The agreement and the disagreement between the two cases provides useful information for understanding the underlying physical mechanism of the delocalization phenomenon of 1DDS driven by the polychromatic perturbations, which we plan to discuss in the future [38].

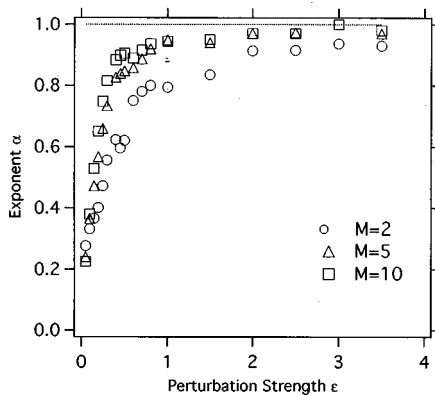


FIG. 9. Perturbation strength dependence of power index α in some cases, $M=2,5,10$.

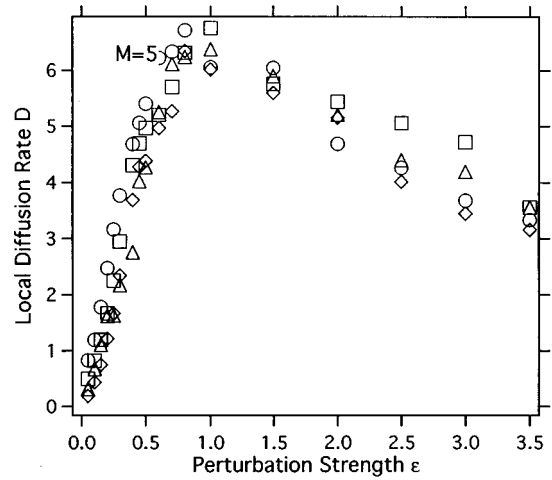


FIG. 10. Perturbation strength dependence of the local diffusion rate for some intervals (100–300, 300–500, and so on) at $M=5$.

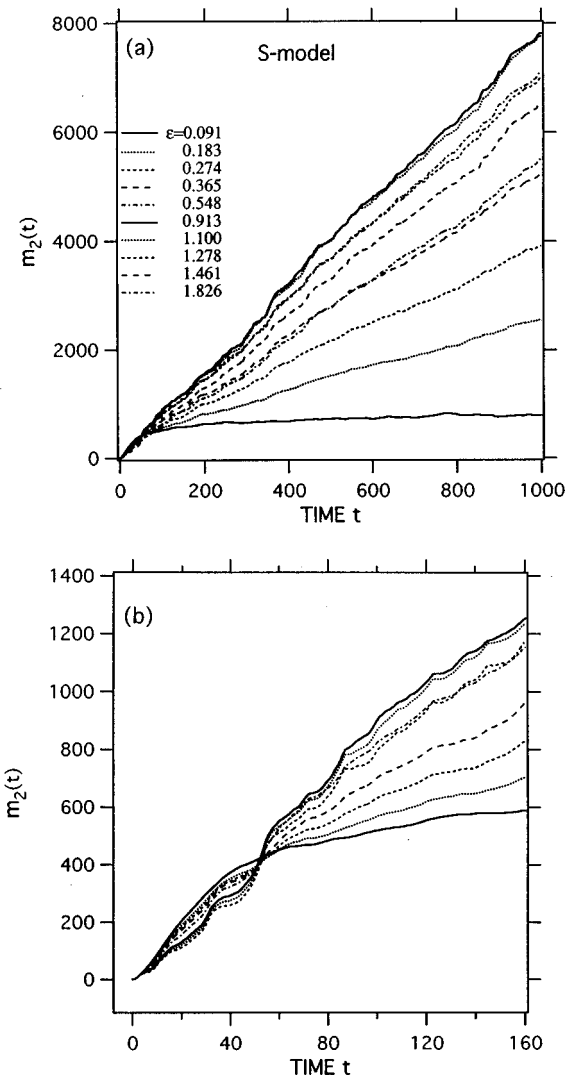


FIG. 11. (a) Time dependence of MSD for stochastic perturbation at some perturbation strength. (b) Expansion of the vicinity of an origin in (a).

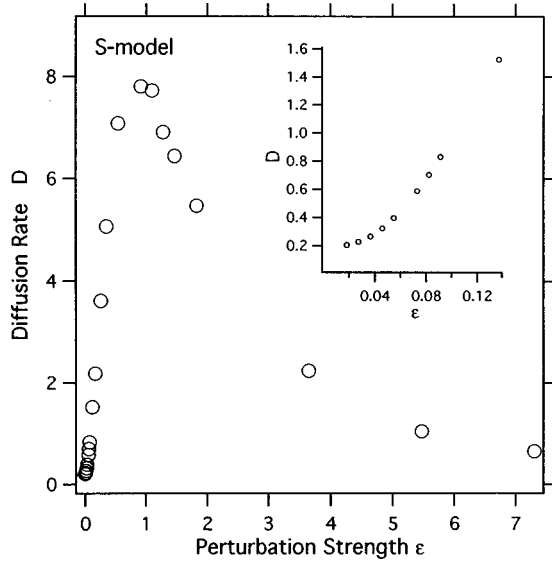


FIG. 12. The perturbation strength dependence of diffusion rate estimated by the MSD data in Fig. 11. (b) The expansion of the vicinity of an origin in (a).

The observation of environment induced decoherence of dynamically localized states in a quantum kicked rotor (QKR) is interesting [39–41]. Moreover, note that some properties of spectra and eigenstates of a band random matrix (BRM) are expected to have statistical properties similar to those of the QKR [42,43]. It has been reported that in the QKR and BRM the strength of noise exceeds some critical value, then it destroys the coherent effect of quantum localization and pure classical diffusion is recovered [37,41]. Quantum diffusion with small diffusion rate can be observed for a smaller noise strength than the critical strength.

On the other hand, although there are interesting preliminary results that subdiffusive behavior for the spread of a wave packet has been found in coupled QKRs with weak coupling strength [23,26], more detailed numerical investigations with adequate accuracy have to be carried out for the high-dimensional QKR and periodically perturbed QKR without any external stochasticity.

D. Scaling properties

The MSD, which obeys the subdiffusion law, approaches rapidly but continuously the normal-diffusion law as M and/or ϵ is increased. In the normal-diffusion regime, we can expect that the distribution function

$$P(n,t) \equiv \langle |\Psi(n,t)|^2 \rangle_{\Omega} \quad (15)$$

evolves in the Gaussian form

$$P(n,t) \propto \exp\{- (n - n_0)^2 / [2\xi(t)^2]\}. \quad (16)$$

On the other hand, the localization occurs at least in the case of $M \leq 1$, in which the wave packet decays in a linear-exponential form [3]

$$P(n,t) \propto \exp\{- |n - n_0| / \xi(t)\}. \quad (17)$$

We are interested in how the time-evolution process of the distribution function changes as the localization process

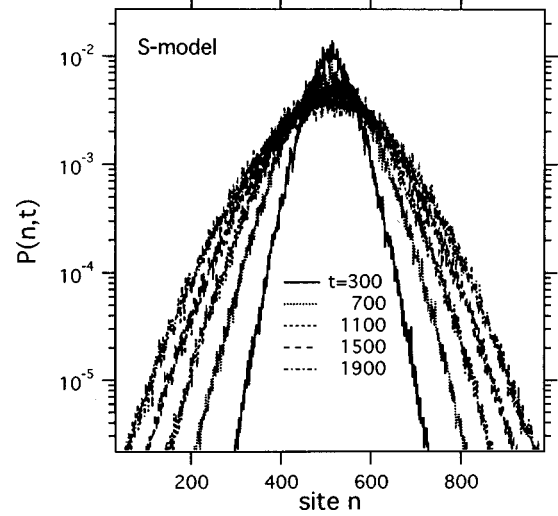


FIG. 13. Some snapshots of the ensemble averaged probability distribution function of S model at the perturbation strength $\epsilon = 0.5$. The ensemble size is 50.

changes into normal diffusion with increases in M and ϵ . In particular, we will show that the time-evolution process of the distribution function obeys a remarkable scaling law in the subdiffusion regime.

First we show typical examples of $P(n,t)$ in the localization regime and in the subdiffusion regime, in comparison with $P(n,t)$ of the S model which obeys the standard Gaussian process. Figures 13 and 14 show some snapshots of $P(n,t)$ for the S model, and for the L model with $M = 0, 2$, and 5. We use 50 samples of spatial disorder to average the distribution function.

Some analytical results have been obtained for steady-state distribution in a continuous 1D disordered model with white noise potential [44]. The shape of the wave packet in the unperturbed case is consistent with the analytical form. Moreover, it has been shown that the analytical expression reproduces the asymptotic average of the wave packet for some quasi-1DDSs well [37].

In the S model the distribution function spreads exactly in the shape of the Gaussian distribution function, and such a behavior, of course, occurs regardless of the perturbation strength. In contrast with this, the distribution function becomes localized and approaches the shape of the linear-exponential decay [Eq. (17)] in the case of $M = 0$. On the other hand, in both cases $M = 2$ and 5, which exhibit the subdiffusion, the wave function spreads, but they seem to have some interpolated shape between Eq. (16) and Eq. (17). Moreover, a remarkable peak remains in the vicinity of the center of the distribution even in the later stage of time evolution (at least up to $T \sim 1900$). The presence of such a peak seems to be strongly correlated with the subdiffusion (and the localization as well). In fact, as normal diffusion is achieved with increase in ϵ and/or M , such a peak disappears.

Next, we seek the mathematical rule underlying the time-evolution process of the $P(n,t)$. In both extreme cases of localization and of normal diffusion, it is evident that the distribution function obeys the scaling rule

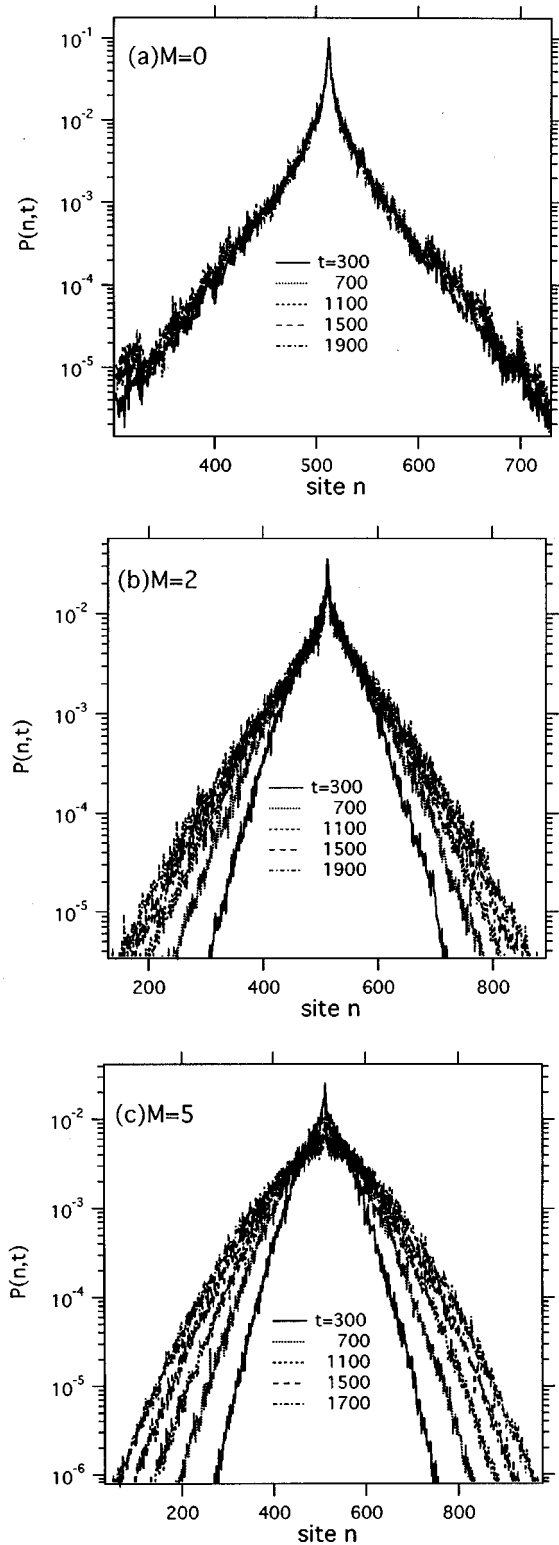


FIG. 14. Some snapshots of the ensemble averaged probability distribution function of L model for some different numbers of frequency (a) $M=0$, (b) $M=2$, (c) $M=5$. The perturbation strength is taken at $\epsilon=0.5$. The ensemble size is 50.

$$P(n, t_2) = \frac{\xi(t_1)}{\xi(t_2)} P\left(\frac{\xi(t_1)}{\xi(t_2)} n, t_1\right) \quad (18)$$

at two arbitrary times t_1 and t_2 in the time domain in which the stationary evolution is achieved. For the sake of simplic-

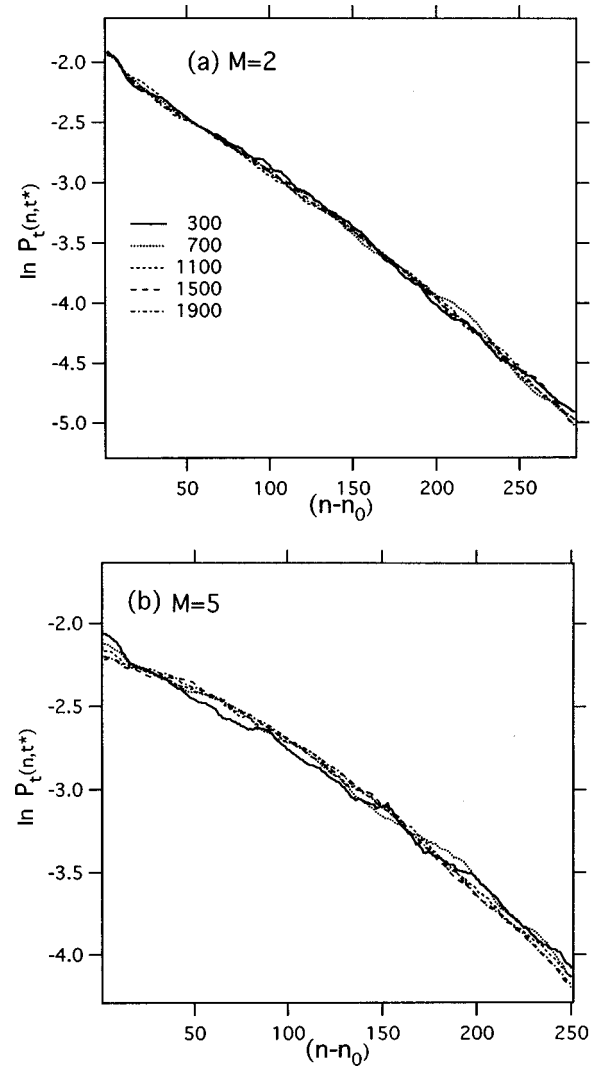


FIG. 15. Semilog plots of the scaled wave functions $P_t(n, t^*)$ for various snapshots in L model for (a) $M=2$, (b) $M=3$, (c) $M=5$. We used a snapshot at $t^*=700$ as a standard distribution. Smoothened data are used to observe the coincidence clearly. Since these distribution functions are symmetric with respect to the center of the distribution, the left parts are omitted.

ity, we henceforth redefine the center of the distribution $n = n_0$ as the origin of the distribution function. We may expect that such a scaling rule can also be extended to the subdiffusion regime. We first examine whether our expectation is valid. To do this examination, we suppose the distribution $P(n, t^*)$ at time $t^*(=700)$ is a standard distribution. If the scaling rule (18) is correct, we can construct the distribution function at t^* from the one at an arbitrary t by setting $t_2 = t^*$ and $t_1 = t$ in Eq. (18). The only information necessary to carry out the procedure is the $P(n, t)$ and MSDs $\xi(t)^2$ and $\xi(t^*)^2$. If such distribution functions, $P_t(n, t^*) \equiv \xi(t^*)/\xi(t) P(\xi(t^*)/\xi(t)n, t)$, made up from $P(n, t)$ at different t 's, coincide with each other, we can prove the presence of the scaling property. In Figs. 15(a)–15(c) we show the semilog plots of the $P_t(n, t^*)$'s obtained at several t 's in the cases of $M=2, 3, 5$. (The perturbation strength ϵ is taken at a fixed value of 0.5 for all data.) All the $P_t(n, t^*)$'s coincide with each other very well, and thus we have to conclude that $P(n, t)$ is represented by a single scaled form,

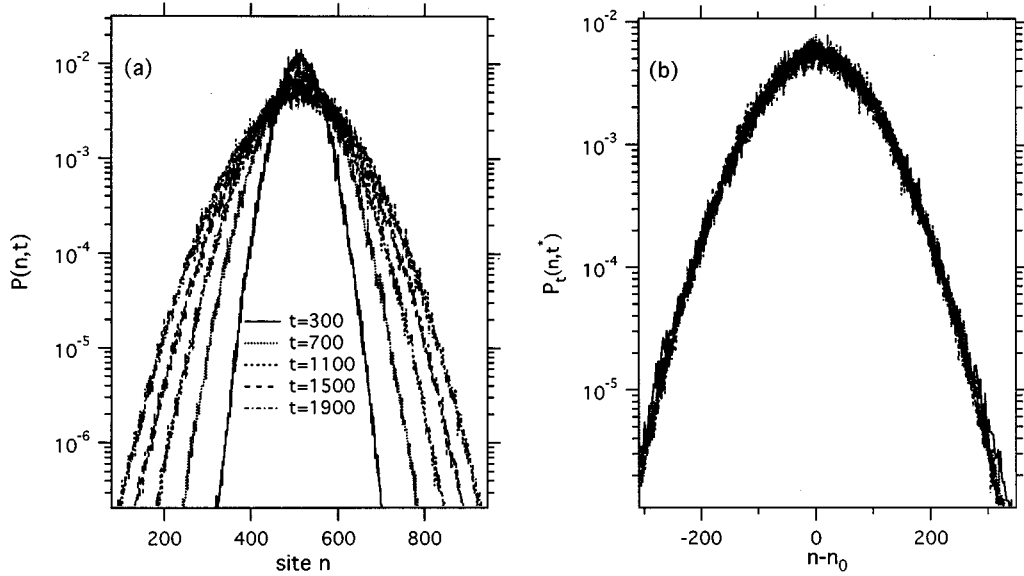


FIG. 16. (a) Some snapshots of the ensemble averaged probability distribution function $P(n,t)$ and (b) the scaled function $P_t(n,t^*)$ ($t^*=700$) of L model for $M=3$, $\epsilon=2.0$. The ensemble size is 50.

$$P(n,t) = \xi(t)^{-1} P_{sc}\left(\frac{n}{\xi(t)}\right). \quad (19)$$

In Fig. 15 smoothed data are used to observe the coincidence clearly. The data at $t=300$ are still in the early stage and thus slightly deviate from the scaled form achieved by the data in the later stages. The time evolution of distribution functions and the scaled functions at different choices of the parameters are also shown in Figs. 16 and 17, where the original data which are not smoothed are displayed. These data also support the above conclusion.

Finally we investigate in more detail the functional form of $P_{sc}(x)$. Let $g(x)$ be the exponent function defined by

$$P_{sc}(x) = e^{-g(x)}. \quad (20)$$

Observing that in the Gaussian limit $g(x) \propto x^2 + \text{const}$, whereas $g(x) \propto |x| + \text{const}$ in the localization limit, we may guess that the function $g(x)$ shows the power-law dependence except for a constant part

$$g(x) - g_0 \propto |x|^\beta, \quad (21)$$

which interpolates the two limiting situations, where the exponent β will take a fractional value between 1 and 2 and g_0 is a certain positive constant. However, as stated above, the scaled distribution function has a sharp peak at the center of the distribution, and the scaled distribution function will be fitted to the power law (20) except for the singular part very close to the central peak. The unknown parameters g_0 and β are decided so that $Q(x, g_0) \equiv \ln\{-\ln P_{sc}(x) + g_0\}$ may fit

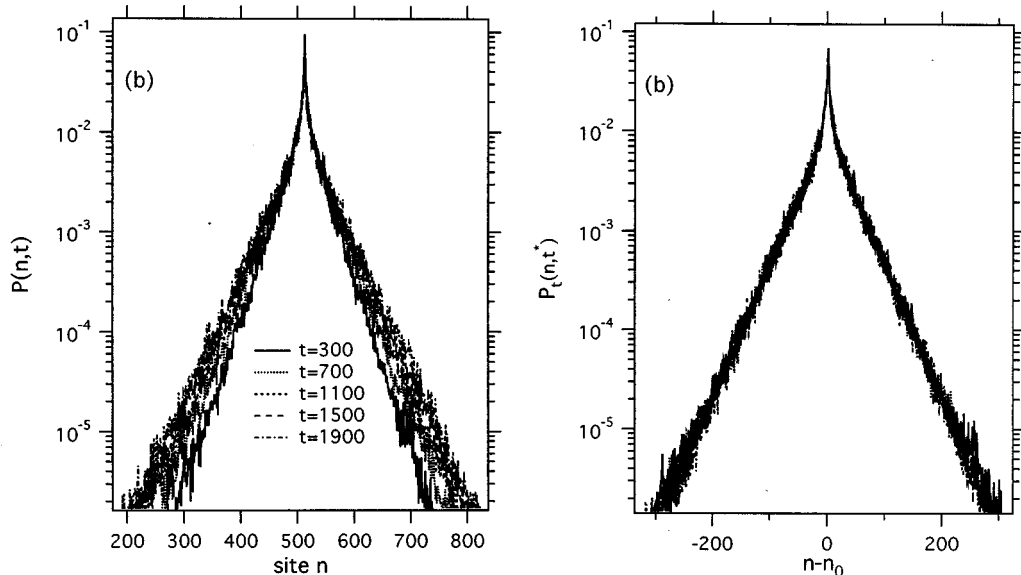


FIG. 17. (a) Some snapshots of the ensemble averaged probability distribution function $P(n,t)$ and (b) the scaled function $P_t(n,t^*)$ ($t^*=700$) of L model for $M=10$, $\epsilon=0.1$. The ensemble size is 50.

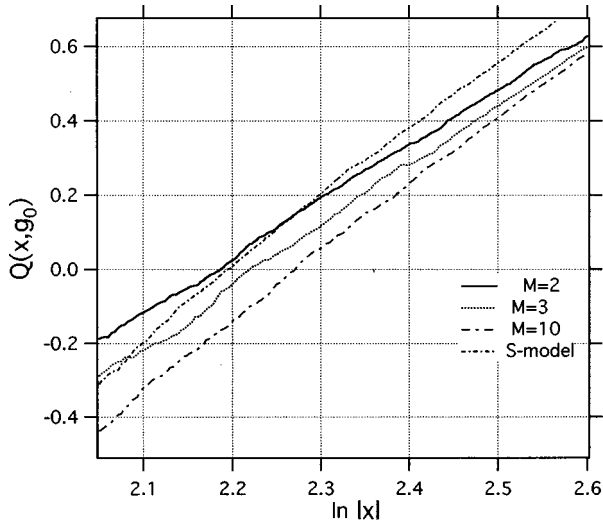


FIG. 18. Best linear fits of the scaled distribution function in the cases of the L model for $M=2, 3, 5$, and S model. We used the value $g_0=2.4$ as the best selection for all cases. We used a snapshot at $t^*=700$ as a standard distribution.

best to the linear function of $\ln|x|$, i.e., $\beta \ln|x| + \text{const}$ except for the range close to the origin. For smaller g_0 , the $Q(x, g_0)$ is concave as a function of $\ln|x|$, whereas it is convex for larger g_0 , and for an optimal g_0 the $Q(x, g_0)$ becomes nicely straight as a function of $\ln|x|$ except for the range close to the origin.

In Fig. 18 we show the best linear fits of the scaled distribution functions in the cases of $M=2, 3, 10$, and S model ($\epsilon=0.5$). The fitting is very nice in the significant region of x , which strongly indicates the validity of the power-law dependence. The precise choice of the exponents β is not very easy, and it is accompanied by some amount of error, but it is evident that as the number M increases (ϵ is fixed) the exponent increases gradually from 1 to the upper bound 2 in the Gaussian limit $M \rightarrow \infty$. Similar behavior occurs when ϵ is increased with the number of colors being fixed ($M \geq 2$). In conclusion, the scaled form of the distribution function is given by the “stretched” Gaussian distribution

$$P_{\text{sc}}(x) \propto \exp\{-\text{const} \times |x|^\beta\}, \quad (22)$$

$$P(n, t) \sim \exp\{-\text{const} \times (|n|/t^{\alpha/2})^\beta\}, \quad (23)$$

except for the range close to $x \sim 0$. Thus the distribution function is specified by the two exponents, i.e., α characterizing the temporal growth of the wave packet, and β characterizing the spatial decay of the wave function. Our scaled distribution function is a unified form which contains the two extreme limits, i.e., the localization ($\alpha=0, \beta=1$) and the normal diffusion ($\alpha=1, \beta=2$) as special cases, and in general interpolates them.

A question arising here is about the relation between the two exponents α and β . If the exponent $\alpha=1$ then we expect that the diffusion process is normal diffusion and so the spatial exponent $\beta=2$, whereas if $\alpha=0$ we expect that the system is localized and thus $\beta=1$. Therefore, the two exponents are not independent and are strongly correlated at least in the normal-diffusion limit and in the localization limit. Such a correlation between the two exponents may also exist

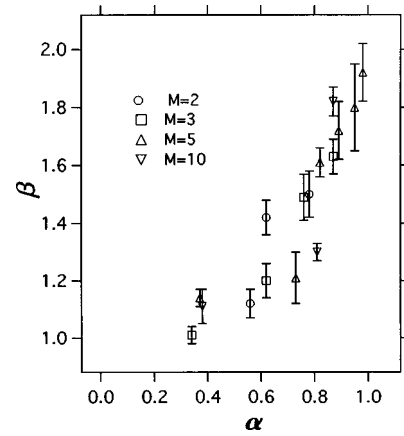


FIG. 19. Plot of (α, β) obtained at various combinations of ϵ and M . Note that $(\alpha, \beta) = (0, 1)$ is the localization limit and $(1, 2)$ is the normal-diffusion limit.

in the intermediate regime where the anomalous diffusion is observed. Figure 19 shows the plot of (α, β) obtained for various combinations of the two independent parameters ϵ and M . The precise determination of β is more difficult than α , and the former is accompanied by some amount of error, but it is evident that the two exponents are strongly correlated in the subdiffusion regime. Because of the numerical errors, it is not convincing that the plots of the two exponents are on a single unique curve. Whether the two exponents are independent or whether one of them is decided by the other is a quite interesting question worth being examined by a more extensive numerical simulation. As has already been mentioned, the data of MSD and of the shape of the probability distribution function are accompanied by a large amount of fluctuation in the subdiffusion regime, and we have to take the ensemble average over a larger number of samples in order to eliminate the numerical errors of the exponents. Moreover, the large fluctuation itself is a very interesting phenomenon inherent in the subdiffusion, which we plan to analyze in more detail in the future.

IV. OTHER MODELS

In the present section we investigate the characteristics of diffusion in the one-dimensional tightly binding models driven by the oscillatory perturbation in ways different from the L model, namely, the AC model and the B model, which have been introduced in Sec. II A.

A. AC model

The characteristics of diffusion of the AC model are very similar to those of the L model. We discuss some details. Figures 20(a)–20(c) show the MSD at the perturbation strength $\epsilon=0.01$. In the monochromatically perturbed case the diffusive behavior saturates at a certain level, and we conclude that the localization is not still destroyed by the monochromatic perturbation. However, the localization length is considerably enhanced by the monochromatic perturbation.

Next we consider polychromatically perturbed cases. We show in Figs. 20(d) and 20(e) the logarithmic plots of MSD vs time. All the data align along straight lines with tangents

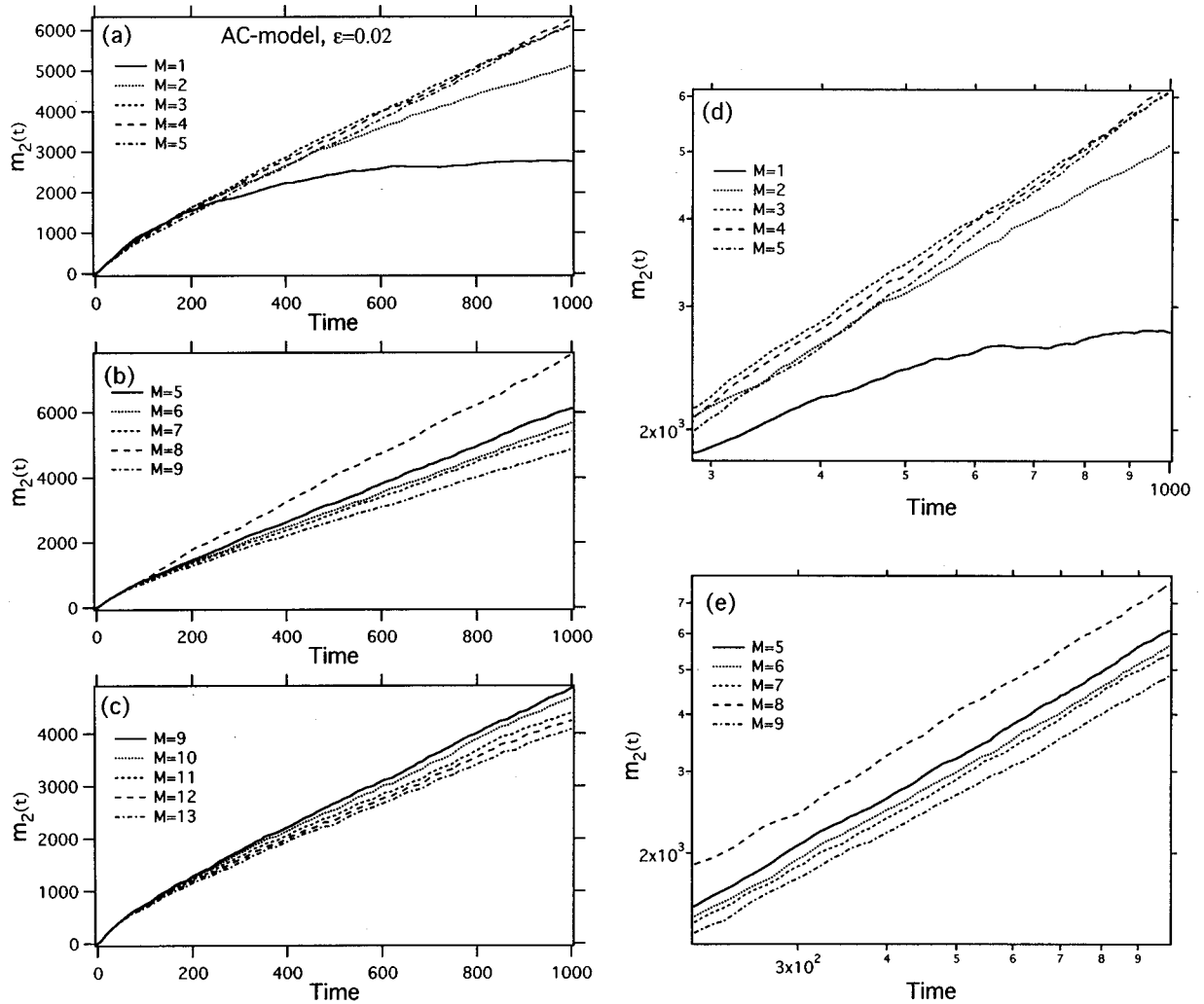


FIG. 20. (a), (b), (c) Time dependence of the MSD in AC model driven by oscillatory perturbation for polychromatic color ($M=1-13$) at some perturbation strength, $\epsilon=0.02$, and (d), (e) its logarithmic plots.

less than 1, and so we may conclude that the MSD obeys the subdiffusion law. Figure 21 is the M dependence of the power index $\alpha(M)$ and coefficient $\ln D(M)$ in Eq. (14), estimated from the data in Fig. 20. The results suggest that normal diffusion is realized in the limit of $M \rightarrow \infty$, as has been recognized in the L model. In conclusion, all the features of the AC model are quite similar to the L model.

B. B model

Without the oscillatory perturbation, the dynamics of the B model exhibits a ballistic motion instead of the localization and thus makes a sharp contrast to the L model. The major interest here is how such a ballistic motion is suppressed and changes into other kinds of motion by introducing the dynamically oscillating random scatterers.

In the numerical simulation of the B model the perturbation strength ϵ is made considerably larger than in the L model because of some technical reasons: at small values of ϵ the wave packet spreads very quickly to reach the boundary of the system because of the ballistic nature of the unperturbed motion, and it is very difficult to observe the stationary stage of the motion with a numerical simulation of a finitely sized model. In practice we fixed the perturbation

strength to the relatively large value $\epsilon=2.0$ and change the number of colors M .

By introducing the oscillatory perturbation, we observed that the ballistic motion changes into either localized or diffusive motion, but there are some qualitatively noticeable differences from the L model. The diffusion rate is in general much larger than that of the L model at the same ϵ and M . Figure 22 shows the logarithmic plots of MSD as a function of time at $M=1,2,\dots,13$. At $M=1$, the ballistic motion seems to be most drastically suppressed: the logarithmic plots of the MSD deviate significantly from a straight line, which strongly indicates a tendency toward the localization. We conjecture that localization occurs in the present case, but the localization length is much larger than the case of the L model and AC model at the same values of M and ϵ .

At M larger than 1 the logarithmic plots of MSD are obviously on the straight line of tangent 1.0, and the subdiffusion regime, which is a remarkable characteristic in the L and the AC models, cannot be observed. The diffusion rate is much larger than that of the L model at the same values of M and ϵ , but it decreases with an increase in ϵ . In the limit of $\epsilon \rightarrow \infty$ the L model approaches the B model, and so the diffusion rates of the two models should coincide asymptotically in this limit.

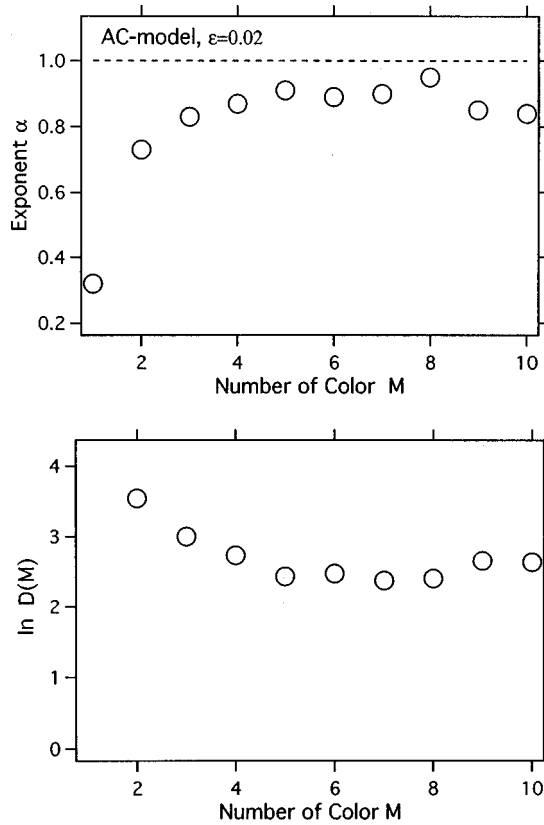


FIG. 21. Number of frequency dependence of (a) the power index α , and (b) coefficient D , estimated from the data in Fig. 20.

V. SUMMARIES AND DISCUSSIONS

We have numerically investigated the time-evolution process of a one-dimensional disordered quantum system driven by an oscillatory perturbation which consists of different frequency components. Any disordered quantum system is not isolated from the influences of other degrees of freedom, and such an effect may drastically change the nature of the disordered system. By adding the oscillatory perturbation we intend to simulate the influences of other dynamical degrees of freedom. We are particularly interested in how the number of degrees of freedom of the perturbation changes the localization effect which is the generic nature of 1DDS. In our model the number of degrees of freedom can easily be controlled by the number M of the different frequency components.

The time evolution of a wave packet is investigated by systematically changing M and the perturbation strength ϵ . The higher-order FFT-symplectic-integrator scheme was used in the numerical computation. The localization is very sensitive to the oscillatory perturbation, and under some general conditions the localization length is much enhanced to a level which cannot be decided by numerical computations. The wave packet diffuses far beyond the localization length of the original 1DDS, and it has been discovered that the diffusion process obeys a unified scaling law characterized by a few characteristic exponents. The results we obtained in the present investigation are summarized as follows.

(1) In the case of the monochromatic perturbation ($M = 1$), a diffusion occurs in an early stage of time evolution, but it is suppressed on a longer-time scale, and the mean

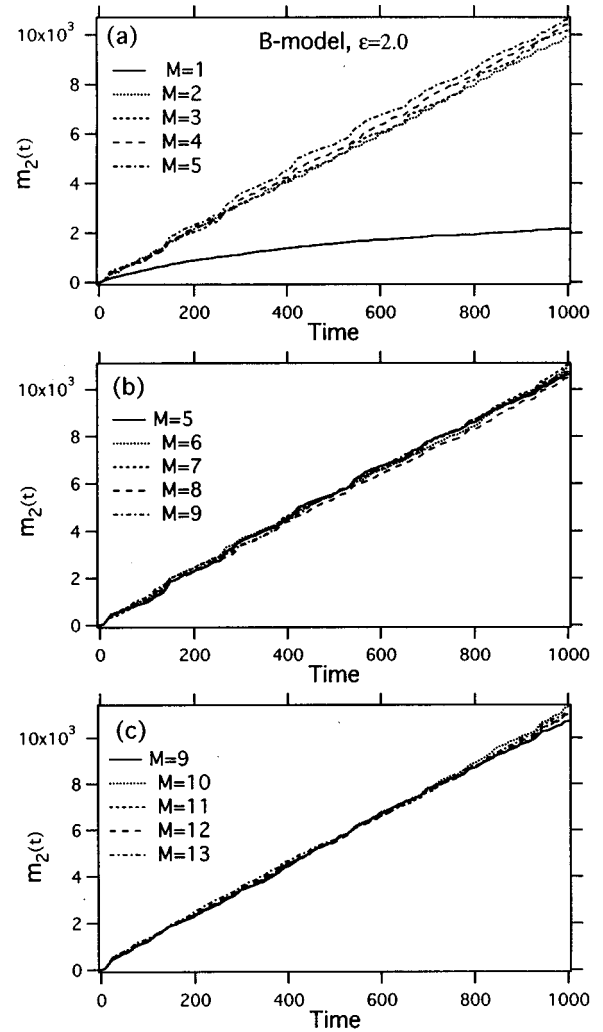


FIG. 22. Time dependence of the MSD in B model driven by oscillatory perturbation for polychromatic color ($M = 1-13$) at the perturbation strength, $\epsilon = 2.0$.

square displacement $\xi(t)^2$ is eventually bounded by a certain finite level. (See Fig. 3.) Thus the localization is not destroyed by the monochromatic perturbation. However, the localization length is enhanced more than the localization length of the unperturbed 1DDS.

(2) In the case of the number $M \geq 2$, diffusive behavior is maintained within the time scale accessible by the numerical simulation. (See Fig. 4.) The diffusion process is not, however, in general the normal diffusion $\xi(t)^2 \propto t$ but the subdiffusion in which the MSD increases as $\xi(t)^2 \propto t^\alpha$. (See Fig. 4.) The characteristic exponent α is between 0 and 1, and as the number M and/or the perturbation strength ϵ increases, the exponent α approaches 1. (See Figs. 5 and 10.)

(3) The subdiffusive behavior of MSD implies the existence of a scaling property in the time-evolution process. Indeed, the distribution function $P(n, t)$ is scaled by $\xi(t)$, which is decided by the exponent α . (See Figs. 15–17.) Further, the scaling function is specified by a new exponent β characterizing the spatial decay of the distribution. (See Fig. 18.) Consequently, the spatiotemporal behavior of the distribution function is characterized by the spatial exponent β and the temporal exponent α in the form of

$P(n,t) \sim \exp\{-\text{const}(|n|/t^{\alpha/2})^\beta\}$ (see Fig. 14), which is a unified scaling distribution containing the two cases, i.e., localization ($\alpha=0, \beta=1$) and normal diffusion ($\alpha=1, \beta=2$) as extreme limits. (See Fig. 19.) The results summarized above have been obtained for the L model. We also examined other kinds of models of the dynamically driven 1DDS.

(4) The diffusion properties of the AC model are very similar to the L model, but the dynamical characteristics of the B model are quantitatively different from the L model. The most remarkable feature is that the subdiffusion regime is not observed, and normal diffusion occurs for $M \geq 2$. (See Figs. 20 and 22.) The fact that the scaling behavior connects the two extreme limits, i.e., localization and normal diffusion, continuously seems to imply that the two seemingly contradictory notions of localization and normal diffusion may be understood in a unified manner by including the oscillatory perturbations.

With the present status of our numerical computation power, it is not very easy to judge whether the subdiffusion is endless or not. However, it is certain that the saturation of subdiffusion could not be observed within a very long-time scale accessible by the numerical simulation. Even though the localization length is finite, it increases very quickly with increase in M and/or ϵ , and we can practically regard the localization length of the asymptotic wave packet as infinite. It will be appropriate to call such a phenomenon *dynamically induced delocalization*, in short, *dynamical delocalization*. The essential unclarified issue is the dynamical mechanism resulting in the scaling behavior in the subdiffusive regime.

A very important fact is that the localization easily turns into a nice diffusive motion if it is driven by a perturbation containing only a small number of frequencies. This fact implies that the localized state of 1DDS has the potential

ability to yield mixing properties which finally lead to a dissipative behavior. This fact provides a hint to elucidate the relationship between the localization and the resistivity (or dissipation), which are both the results of the scattering by irregularly distributed impurities [9]. In short, the localized state is very close to a mixing state which has the ability of losing the initial memory. Such a potential for the mixing in our system is very similar to the characteristic of a quantum chaos system [20,28], although, as discussed in the Introduction, some basic differences may exist between the two systems.

It is worth to noting that the scaled evolution of the distribution function (23) is also reported in a classical diffusion system [45–47]. In particular, it is very interesting that the same form of the non-Gaussian probability distribution has been obtained for the classical Brownian particles with long memory effect on the fractal medium [46,47]. In these cases the exponents corresponding to α and β are directly connected to the exponents of the spatial correlation of scatterers and of the temporal correlation of the random forces, which are both explicitly assumed in the model system. In our case, no such explicit assumption had been done in the model system, and the scaling behavior is self-generated in the system.

ACKNOWLEDGMENTS

One of the authors (H.Y.) wishes to thank Professor M. Goda for useful discussions. The numerical calculations were carried out on the supercomputer at Ristumeikan University. The present work is partially supported by a Grant-in-Aid for Scientific Research “Chemistry of small many body system” provided by the Ministry of Education, Science and Culture, Japan.

-
- [1] For a recent review, see B. Kramer and A. MacKinnon, Rep. Prog. Phys. **56**, 1469 (1993), and references therein.
- [2] See, for example, P. Sheng, *Introduction to Wave Scattering, Localization, and Mesoscopic Phenomena* (Academic Press, New York, 1995).
- [3] K. Ishii, Prog. Theor. Phys. Suppl. **53**, 77 (1973).
- [4] D. J. Thouless, Phys. Rev. Lett. **47**, 92 (1981).
- [5] Throughout this paper we use the term “localization length” to express the spread of the asymptotic localized wave packet. In the case of a nonperturbed disordered system, the spread of the initially localized wave packet is directly related to the localization length of the eigenstates.
- [6] P. Sebbah, D. Sornette, and C. Vanneste, Phys. Rev. B **48**, 12 506 (1993); H. Yamada and M. Goda, Phys. Lett. A **194**, 279 (1994); A. Sain and A. Mookerjee, Mod. Phys. Lett. B **8**, 195 (1994).
- [7] E. Doron and S. Fishman, Phys. Rev. Lett. **60**, 867 (1988).
- [8] H. Yamada, K. Ikeda, and M. Goda, Phys. Lett. A **182**, 77 (1993).
- [9] H. Yamada and K. S. Ikeda, Phys. Lett. A **222**, 76 (1996).
- [10] A. O. Caldera and A. J. Leggett, Ann. Phys. (N.Y.) **149**, 374 (1983); E. Shimshoni and Y. Gefen, *ibid.* **210**, 16 (1991); Y. C. Chen and J. L. Lebowitz, Phys. Rev. Lett. **69**, 3559 (1992).
- [11] J. P. Bouchaud, D. Touati, and D. Sornette, Phys. Rev. Lett. **68**, 1787 (1992).
- [12] H. Haken and G. Strobl, Z. Phys. **262**, 135 (1973); H. Ezaki and F. Sibata, Physica A **187**, 267 (1992).
- [13] A. M. Jayannavar, Phys. Rev. E **48**, 837 (1993).
- [14] J. S. Howland, Math. Ann. **207**, 315 (1974).
- [15] N. F. Mott and E. A. Davies, *Electronic Processes in Non-Crystalline Materials* (Clarendon, Oxford, 1979).
- [16] R. Kubo, Can. J. Phys. **34**, 1274 (1956); A. D. Greenwood, Proc. Phys. Soc. London, Sect. A **68**, 589 (1957).
- [17] M. Wilkinson, J. Phys. A **21**, 4021 (1988); **24**, 2615 (1991).
- [18] M. Wilkinson, J. Phys. A **23**, L957 (1990); M. Wilkinson and E. J. Austin, Phys. Rev. A **46**, 64 (1992).
- [19] A. Stern, Y. Aharanov, and Y. Imry, Phys. Rev. A **41**, 3436 (1991).
- [20] M. Toda, Physica D **59**, 121 (1992); Prog. Theor. Phys. Suppl. **116**, 379 (1994).
- [21] A. M. Jayannavar, Solid State Commun. **73**, 247 (1990).
- [22] S. Fishman, D. R. Grempel, and R. E. Prange, Phys. Rev. Lett. **49**, 509 (1982).
- [23] M. Toda, S. Adachi, and K. Ikeda, Prog. Theor. Phys. Suppl. **98**, 323 (1989).
- [24] G. Casati, I. Guarneri, and D. L. Shepelyansky, Phys. Rev. Lett. **62**, 345 (1989).

- [25] G. Casati, I. Guarneri, M. Leschanz, D. L. Shepelyansky, and C. Sinha, *Phys. Lett. A* **154**, 19 (1991).
- [26] H. Kubotani, T. Okamura, and M. Sakagami, *Physica A* **214**, 560 (1995).
- [27] M. Sakagami, H. Kubotani, and T. Okamura, *Prog. Theor. Phys.* **95**, 703 (1996).
- [28] K. Ikeda, *Ann. Phys. (N.Y.)* **227**, 1 (1993).
- [29] F. Neri, University of Maryland technical report, 1988.
- [30] H. Yoshida, *Phys. Lett. A* **150**, 262 (1990).
- [31] H. Raedt, *Computer Physics Report* (North-Holland, Amsterdam, 1987).
- [32] H. Frauenkron and P. Grassberger, *Int. J. Mod. Phys. B* **5**, 37 (1994).
- [33] K. Takahashi and K. Ikeda, *J. Chem. Phys.* **99**, 8680 (1993).
- [34] F. Borgonovi and D. L. Shepelyansky, *Nonlinearity* **8**, 877 (1995).
- [35] F. Borgonovi and D. L. Shepelyansky, *Phys. Rev. E* **51**, 1026 (1995).
- [36] E. Diez, R. Gomez-Alcala, F. Dominguez-Adame, A. Sanchez, and G. P. Berman, *Phys. Lett. A* **240**, 109 (1998); *Phys. Rev. B* **58**, 1146 (1998).
- [37] F. M. Izrailev, T. Kottos, A. Politi, S. Ruffo, and G. Tsironis, *Phys. Rev. E* **55**, 4951 (1997).
- [38] H. Yamada and K. S. Ikeda (unpublished).
- [39] E. Ott, T. M. Anotonsen, and J. D. Hansen, *Phys. Rev. Lett.* **53**, 2187 (1984); S. Adachi, M. Toda, and K. Ikeda, *ibid.* **61**, 655 (1988).
- [40] T. Dittrich and R. Graham, *Ann. Phys. (N.Y.)* **200**, 363 (1990).
- [41] H. Ammann, R. Gray, I. Shvarchuck, and N. Christensen, *Phys. Rev. Lett.* **80**, 4111 (1998).
- [42] Y. V. Fyodrov and A. D. Mirlin, *Int. J. Mod. Phys. B* **8**, 3795 (1994).
- [43] F. M. Izrailev, *Chaos Solitons Fractals* **5**, 1219 (1995).
- [44] A. A. Gogolin, *Zh. Eksp. Teor. Fiz.* **71**, 1912 (1976) [*Sov. Phys. JETP* **44**, 1003 (1976)].
- [45] M. Goda, T. Okabe, H. Yamada, and M. Kobayashi, *J. Phys. Soc. Jpn.* **63**, 2841 (1994).
- [46] K. G. Wang, L. K. Dong, X. F. Wu, F. W. Zhu, and T. Ko, *Physica A* **203**, 53 (1994).
- [47] A. Aharony and A. B. Harris, *Physica A* **205**, 335 (1994).